Chapter 1

FeAl Intermetallic Alloy: Its Heat-Resistant and Practical Application

Janusz Cebulski and Dorota Pasek

Additional information is available at the end of the chapter

http://dx.doi.org/10.5772/intechopen.73184

Abstract

Intermetallic phases, as a group of materials which have a great practical importance, both in the past and in the present day, are subject of research on the basis of physicochemical and mechanical properties. The presented studies were conducted for Fe40Al5Cr0.2TiB intermetallic alloy, their purpose was to determine the corrosion resistance of this alloy in an oxidizing environment, at temperatures up to 1373 K. The test material was made of Fe40Al5Cr0.2TiB intermetallic alloy after plastic processing. The kinetics of corrosion, allotropic variants according to the temperature of the process and the surface condition after corrosion were determined during the study. Based on the results obtained, the verification was performed under operating conditions. Taking into account the properties of the FeAl alloys, the working conditions and material requirements of turbochargers, studies have been undertaken to determine the possibility of the use of Fe40Al5Cr0.2TiB intermetallic alloys for components of the hot turbocharger of the automobile with compression ignition engines. The components of the hot turbocharger parts were used from the test material. The tests distance of turbocharger was 80,000 km.

Keywords: FeAl, corrosion, high temperature, application, Al_2O_3 layer

1. Introduction

Introducing the new materials to industrial practice enables us to build more and more durable and reliable components for machines and equipment that are suitable for use in high temperature and other special conditions. Undoubtedly, this group of innovative and advanced construction materials introduced over the past 30 years includes intermetallic alloys [1] The wide interest in these alloys is mainly due to their unique properties, which in particular include: excellent oxidation, carburizing and sulphate resistance, good corrosion resistance in seawater and melted salts, high resistivity at room temperature (which also increases with

the increase of temperature), as well as high abrasion, erosion and cavitation resistance [2–4]. So much interest in FeAl alloys is due to the fact that during the high temperature processes in the oxidizing atmospheres a protective layer of aluminum oxide is formed on the surface of these materials forms. The layer prevents the degradation of the metallic core. These materials can therefore be used as construction material for working in the atmospheric industrial gases, contaminated with SO_2, O_2 and steam [5].

Bystrzycki and others asserted that a set of favorable properties induces the use of intermetallic alloys as a material working at elevated temperatures in industrial atmosphere. The limitation may, however, be the fragility of these materials [6].

The structure of the alloy is stable however the presence of a pro-eutectoid phase in FeAl leads to a deterioration in the creep resistance [7].

As one of the major limitations of the practical application of FeAl alloys is their low plasticity (which makes it impossible to process with conventional methods). In the first step, FeAl alloys were focused on the feasibility of alloys. The result of this work was a doctoral thesis entitled "Ways to increase the plasticity of the alloy on the matrix of FeAl" [8]. The positive results of the conducted research became the inspiration for further research and development of these materials. The result of the study was the determination of corrosion resistance in a liquid environment, but above all resistance to high temperature gas corrosion. The next step was to verify the results obtained under real-life conditions in turbocharged performance tests where some components were made from FeAl [9, 10]. Alloys of aluminum and iron intermetallic compounds are considered to be future-proof materials for applications in environments with high temperature corrosion, due to their good oxidation resistance (especially in an environment containing sulfur and chlorine). This has been confirmed by the results of the research presented in this paper.

The initial development of research concerning of the Fe-Al intermetallic alloys was aimed at modifying them with suitable alloying elements, such as zirconium, yttrium, boron, manganese, chromium, vanadium, titanium, cobalt and nickel. The research of modified intermetallic alloys with a variety of modifying elements has been conducted by numerous research centres around the world. It has been found that the most effective additives that improve the strength of intermetallic alloys at elevated temperatures and also plasticity and corrosion resistance both for isothermal and cyclic oxidation were: zirconium, boron and fine dispersion of Y_2O_3. Furthermore, the positive effects of alloying additives, both in oxygen and aggressive oxygen and sulfur-containing gas mixtures, on the kinetics of oxidation of intermetallic alloys have been found. The results, obtained by numerous authors, clearly demonstrate the slowdown of the process of the Al_2O_3 scale development due to the modification of the FeAl phase with the appropriate amount of the element. The addition of Cr and Ti results in an increasing of the Fe-Al oxidation rate during the early stages of the reaction, but these additives have improved the adhesion of the scale and the morphology. In addition, they reduced the reaction rate for long periods [11–13].

For the FeAl alloys, elements of bathtubs for bath aluminizing and grate bars for furnaces (which have successfully passed long-term operating tests at 1273 K) are already being made [4]. Practical applications also include intermetallic (FeAl) pallets and racks for furnaces used in heat-chemical treatment as well as rails for roller hearth furnaces and rolls for transporting hot rolled steel sheets [1, 4].

2. Oxidation kinetics and Al_2O_3 morphology after heat-resistance tests

The test material was made of Fe40Al5Cr0.2TiB intermetallic alloy after plastic processing. The smelting process was carried out under vacuum. To homogenize the chemical composition, homogenizing annealing was performed at a temperature of 1323 K for 72 h. The resulting material was plastically extruded to improve the mechanical properties of the alloy for practical application. Fine-tuning was carried out using a proprietary technology that is patentable. The developed method makes it possible to perform reprocessing of hard-to-change materials in a repetitive manner without cracks [14].The chemical composition of the test alloy is shown in **Table 1**.

The oxidation kinetics of the Fe40Al5Cr0.2TiB intermetallic alloy at 1173, 1223, 1273 and 1373 K for 500 h is shown in **Figures 1** and **2**. The processes of complex diffusion in the Fe40Al5Cr0.2TiB intermetallic alloy and the aluminum oxide layer determine the speed of the process. The kinetics studies (**Figures 1** and **2**) show that the process is parabolic in accordance with the relation $dX/dt = k'_p(t)/X$. The measured rates of reaction did not strictly reflect this law, i.e. at constant temperature $k'_p = f(t) \neq const$ deviations from the standard parabolic equation result from the formation of different Al_2O_3 oxide variants, grain growth and / or formation of mixed oxides that appear during the oxidation reaction. Thus, in spite of the above limitations, it is convenient to approximate the reaction rates to the classical formula (Eq. (1)):

$$x^2 - layer\ thickness,\ cm^2 \quad 2k'_p - constant\ rate\ of\ oxidation,\ \frac{cm^2}{s} \quad t - time,\ s \tag{1}$$

Table 2 shows constants of the oxidation rate for the respective process temperatures, values of which correspond to the parabolic oxidation course (**Figures 1** and **2**).

The research on corrosion products made with scanning electron microscope is presented in **Figures 3–10**. The type of oxides on the surface of oxidized samples was determined by X-ray phase analysis. The results are shown in **Figures 11–13**. At a temperature of 1173 K, the α and θ form of Al_2O_3 oxides were observed (**Figure 11**). After oxidation at a temperature of 1273 K, a small amount of metastable $\theta - Al_2O_3$ and a stable $\alpha - Al_2O_3$ form of oxides were observed (**Figure 12**). Only stable α-Al_2O_3 is present at 1373 K (**Figure 13**). The growth rate of Al_2O_3 scale, in the palaces where it has lost contact with the alloy, is similar to places that where the contact remains. This phenomenon occurs because the rate of evaporation of aluminum from the surface of the metallic phase and its transport in the gas phase towards the inner surface of the scale is faster than diffusion of oxygen through the Al_2O_3 scale. The whiskers appear on the surface of Al_2O_3 scale. This effect is related to the presence of compression stresses in the oxide, which are formed under isothermal conditions following the transverse growth phenomenon. Despite the presence of Fe and Cr in the alloys, the created oxides of these metals

Fe40Al5Cr0.2TiB	Fe	Al	Cr	Ti	B
% Mass	68.21	23.66	5.77	0.15	0.015

Table 1. Chemical composition Fe40Al5Cr0.2TiB alloy.

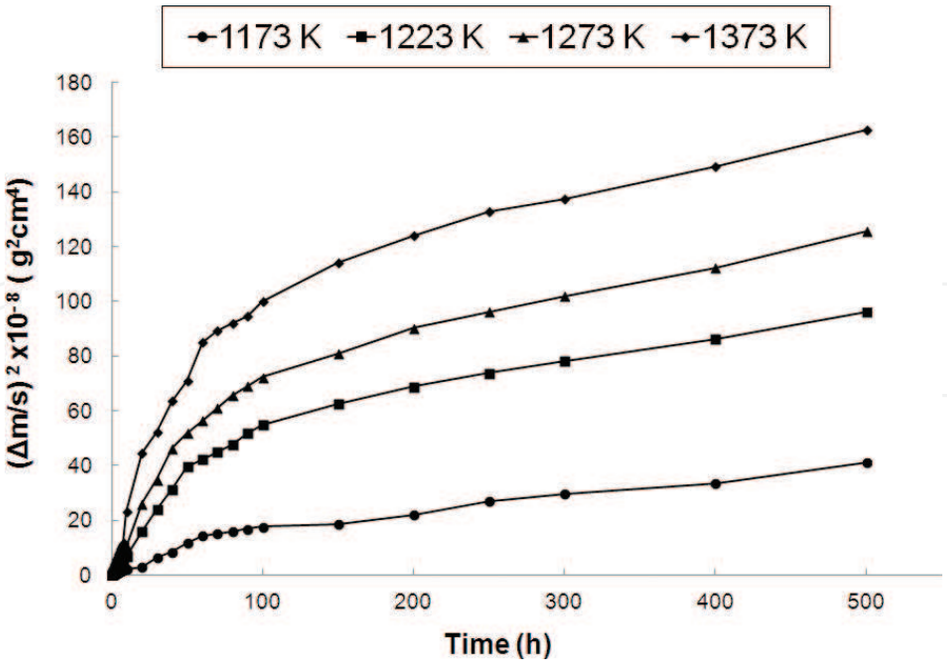

Figure 1. The total weight gain (sample + chips oxide in the crucible) measured after oxidation.

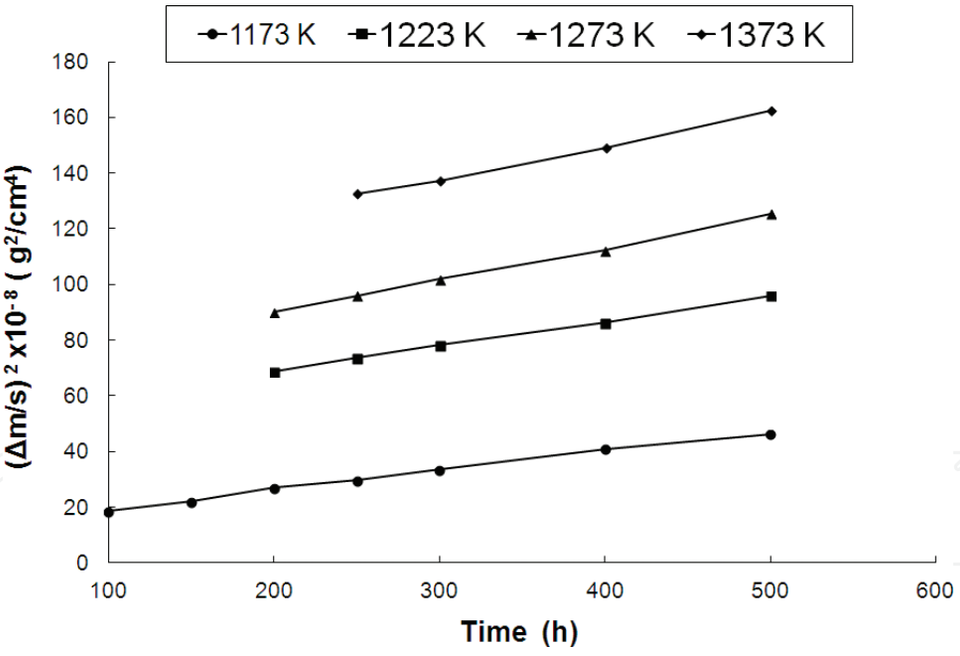

Figure 2. The change in mass intermetallic alloy Fe40Al5Cr0.2TiB in time to 500 h in parabolic coordinates.

have several orders of magnitude higher compressibility decomposition than the oxides forming the protective scale of Al_2O_3. For this reason, Al in the Fe40Al5Cr0.2TiB intermetallic alloy can be selectively oxidized to stable form of Al_2O_3 oxides on the melt surface. From a thermodynamic point of view, the only protective oxide that is likely to form as a stable layer on the Fe40Al5Cr0.2TiB intermetallic alloy is Al_2O_3 [15].

Temperature [K]	k_p'' [$g^2 \cdot cm^{-4} \cdot s^{-1}$]
1173	$1.93 \cdot 10^{-13}$/100–500 h
1223	$2.51 \cdot 10^{-13}$/200–500 h
1273	$3.26 \cdot 10^{-13}$/200–500 h
1373	$3.30 \cdot 10^{-13}$/250–500 h

Table 2. Kp″ constant values for the Fe40A5Cr0.2TiB intermetallic alloy.

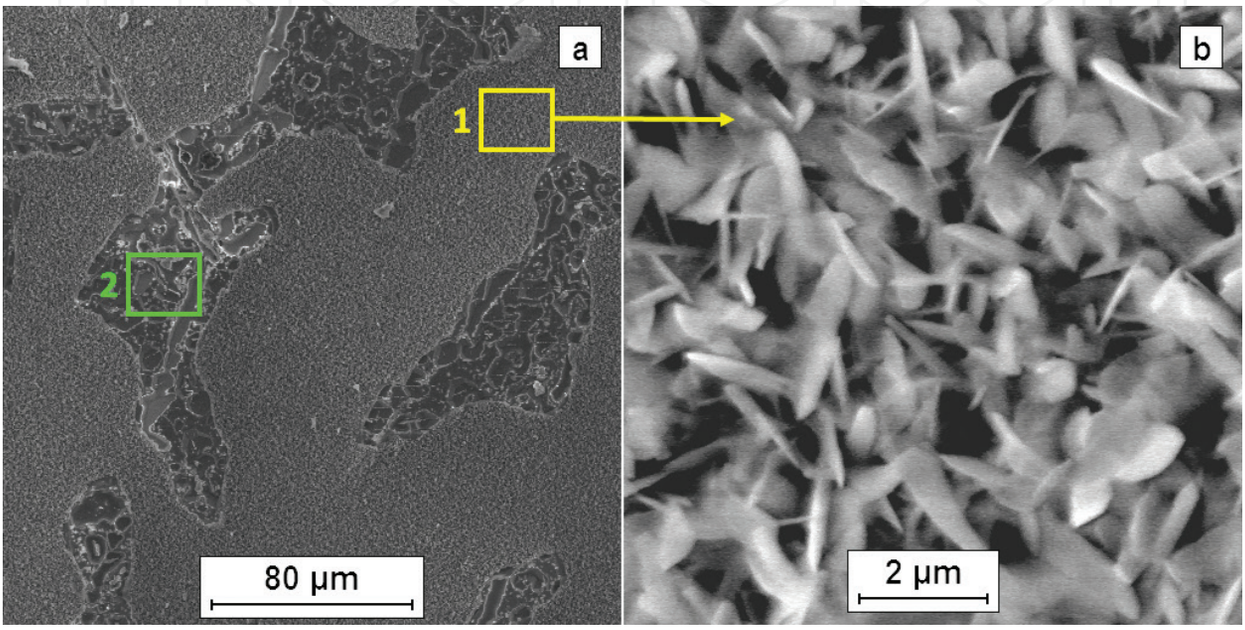

Figure 3. The surface condition of the sample after the corrosion tests at 1173 K for 100 h: a – oxidized surface, b – formed on the surface morphology of the oxide.

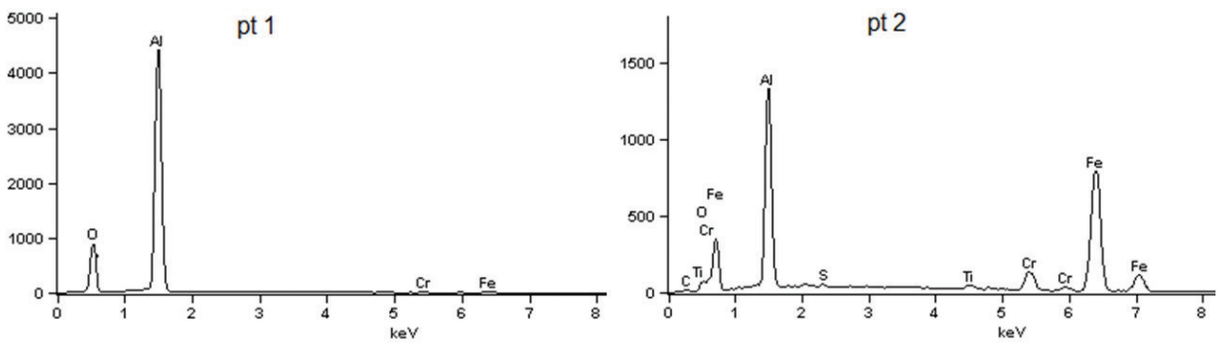

Figure 4. X-ray microanalysis of the chemical composition of the areas indicated on the sample surface after corrosion research at 1173 K for 100 h.

The structure and growth mechanism of the protective Al_2O_3 scale on heat-resistant alloys depends to a great extent on the type of metal in the matrix. Alloys on the FeAl intermetallic phase throughout the entire temperature range remain single phase. For this reason, the Al_2O_3

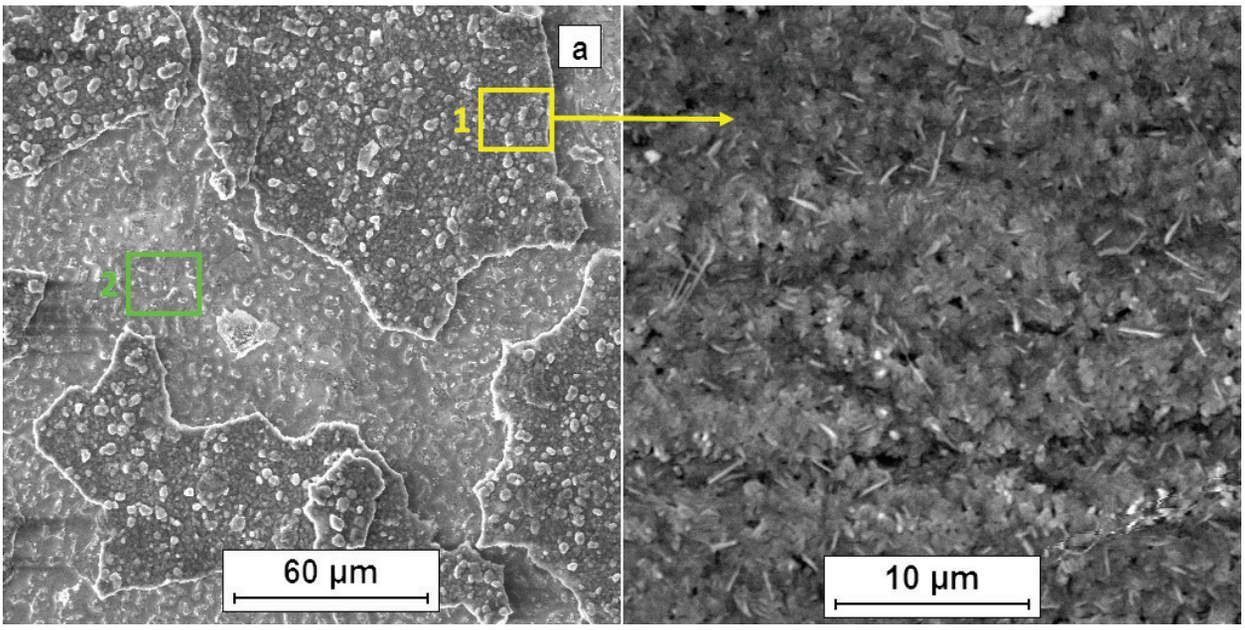

Figure 5. The surface condition of the sample after the corrosion tests at 1223 K for 100 h: a – oxidized surface, b – formed on the surface morphology of the oxide.

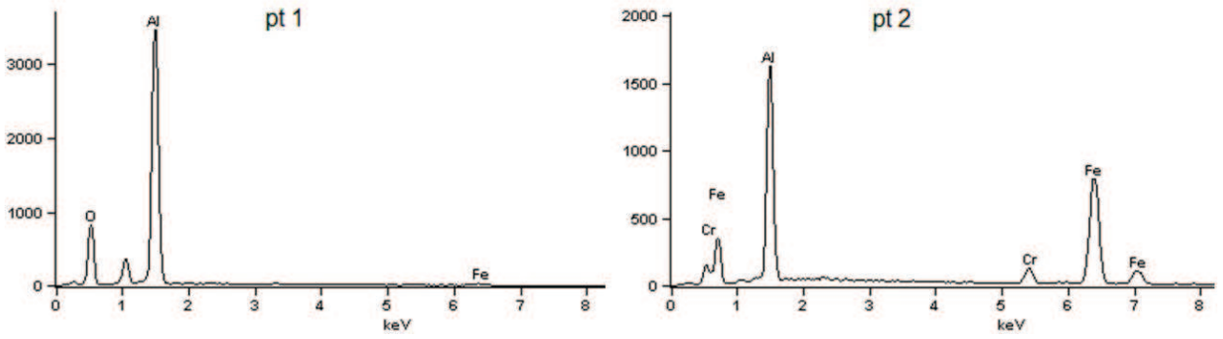

Figure 6. X-ray microanalysis of the chemical composition of the areas indicated on the sample surface after corrosion research at 1223 K for 100 h.

layer is formed throughout its surface at the time of contact of the hot metallic phase with oxygen, regardless of temperature.

The thermal expansion of the alloy affects the level of stress that forms between the oxide and the metallic phase during temperature changes. Relaxation of these stresses can occur when the oxide layer comes off the metallic substrate.

The phase composition of the Al_2O_3 scale, which is formed on the alloys and intermetallic phases on the iron matrix, is influenced by: their chemical composition, the crystallographic structure of the metallic substrate and the temperature at which the oxidation process is carried out. Within the temperature range of 1073–1223 K, in the initial oxidation state, on the surface of many iron alloys, especially the FeAl intermetallic phase, an increase in metastable alumina θ, γ and δ is observed. After a period of time, a protective layer from the α-Al_2O_3 phase is produced. The addition of chromium to the FeAl alloy accelerates the phase transformation $\theta \rightarrow \alpha$ and increases its corrosion resistance [16–18].

http://dx.doi.org/10.5772/intechopen.73184

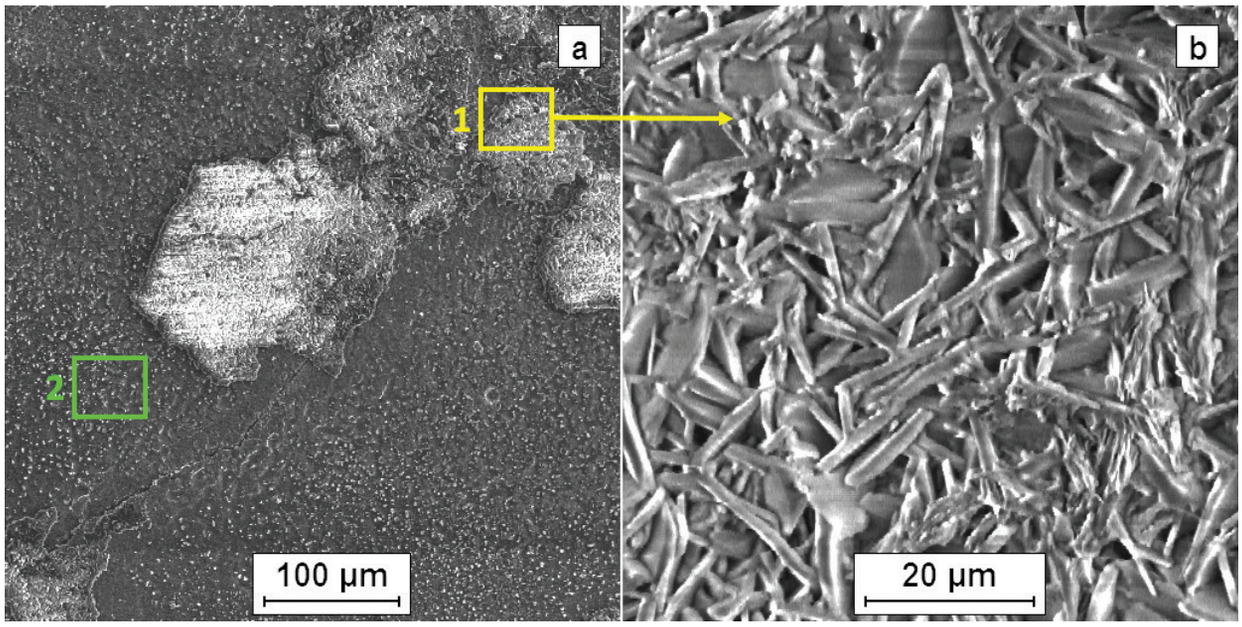

Figure 7. The surface condition of the sample after the corrosion tests at 1273 K for 100 h: a – oxidized surface, b – formed on the surface morphology of the oxide.

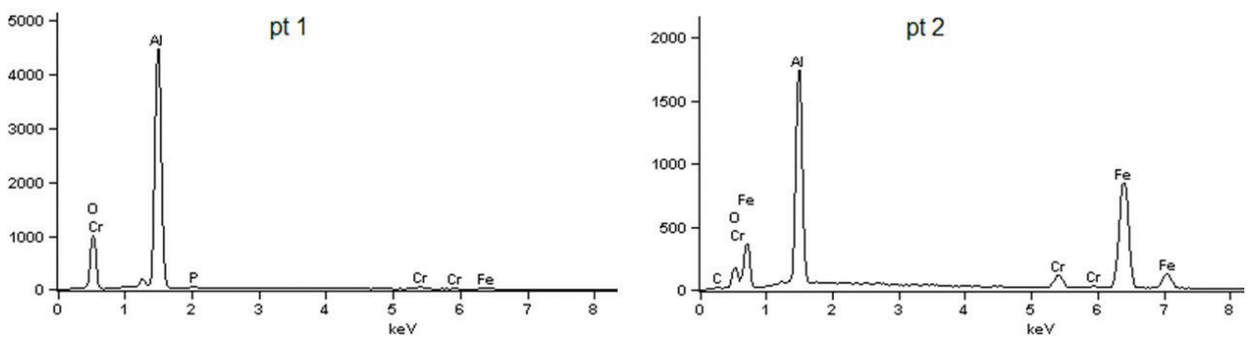

Figure 8. X-ray microanalysis of the chemical composition of the areas indicated on the sample surface after corrosion research at 1273 K for 100 h.

One hypothesis assumes that the growth of metastable phases is related to the phenomenon of epitaxia.

Most of the metallic phases as well as metastable alumina crystallize in the regular grid, whereas alumina – in the hexagonal network. The growth velocity of the θ-Al_2O_3 phase is larger by one order of magnitude than in the case of α-Al_2O_3 phase, and its increase occurs as a result of core metal diffusion and depends on the concentration of vacancies in the cation subnetwork. The period of time required to form the continuous α-Al_2O_3 layer is reduced with increase of oxidation temperature [19].

The morphology of Al_2O_3 oxides varies depending on the process temperature: from the needles appearing at 1173 K to the oxides in the form of grains at 1373 K.

The θ-Al_2O_3 phase grows on FeAl alloys in the form of lamellar grains allowing the external surface of the scale to become strongly developed. Transformation of metastable alumina phases into the α-Al_2O_3 phase starts at the metal-oxide border [18, 19]. This transformation is

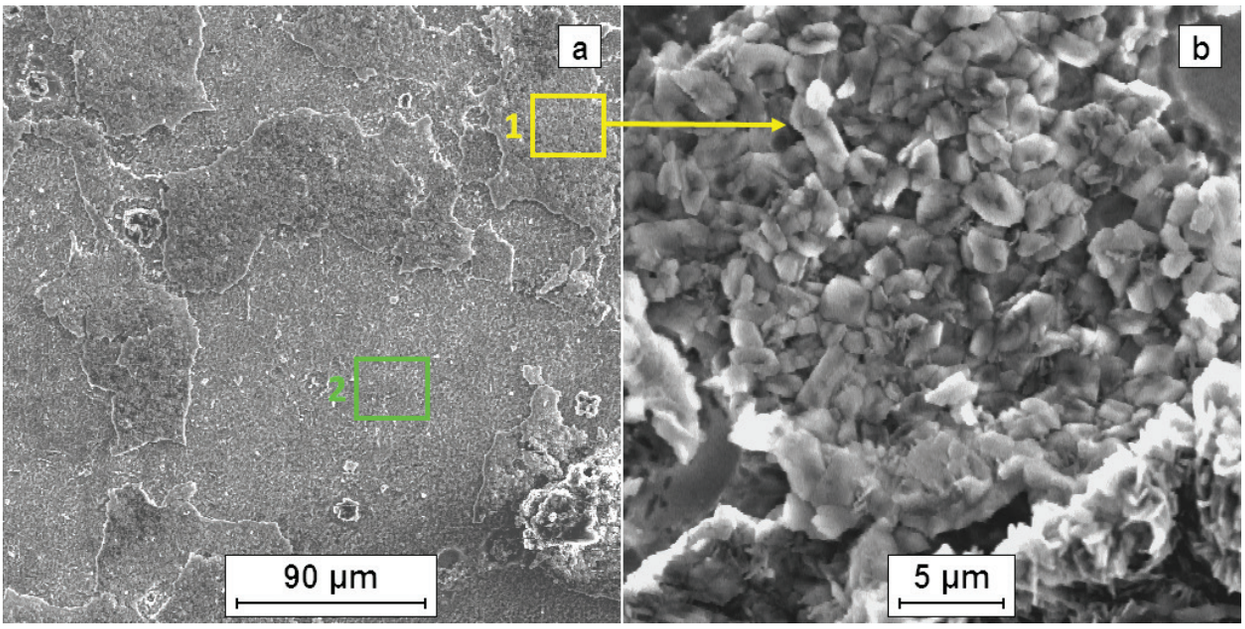

Figure 9. The surface condition of the sample after the corrosion tests at 1373 K for 100 h: a – oxidized surface, b – formed on the surface morphology of the oxide.

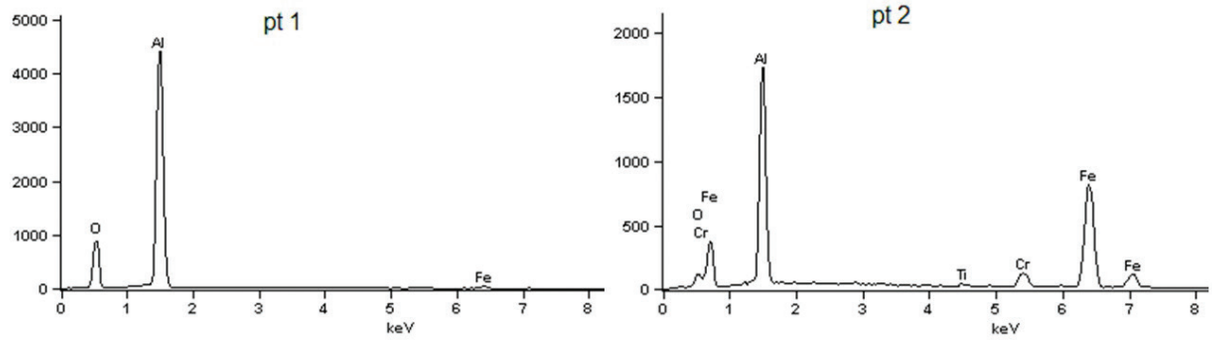

Figure 10. X-ray microanalysis of the chemical composition of the areas indicated on the sample surface after corrosion research at 1373 K for 100 h.

accompanied by a reduction in the volume of the oxide phase, which results in tensile stresses in the layer. The relaxation of these stresses results in numerous microcracks in which the new alumina is built up. Such microcapsules, filled with oxides, form a characteristic grid on the surface of the scale, which resembles a spider web [20, 21].

The growth of α-Al2O3 scale occurs as a result of the predominant, intra-articular transport of oxygen across the grain boundaries in the oxide. Because of low concentration of point defects in the α-Al_2O_3 phase, the aluminum and oxygen network diffusion in this oxide is not taken into account in the balance of mass transport through the layer of corrosion product [22, 23].

http://dx.doi.org/10.5772/intechopen.73184

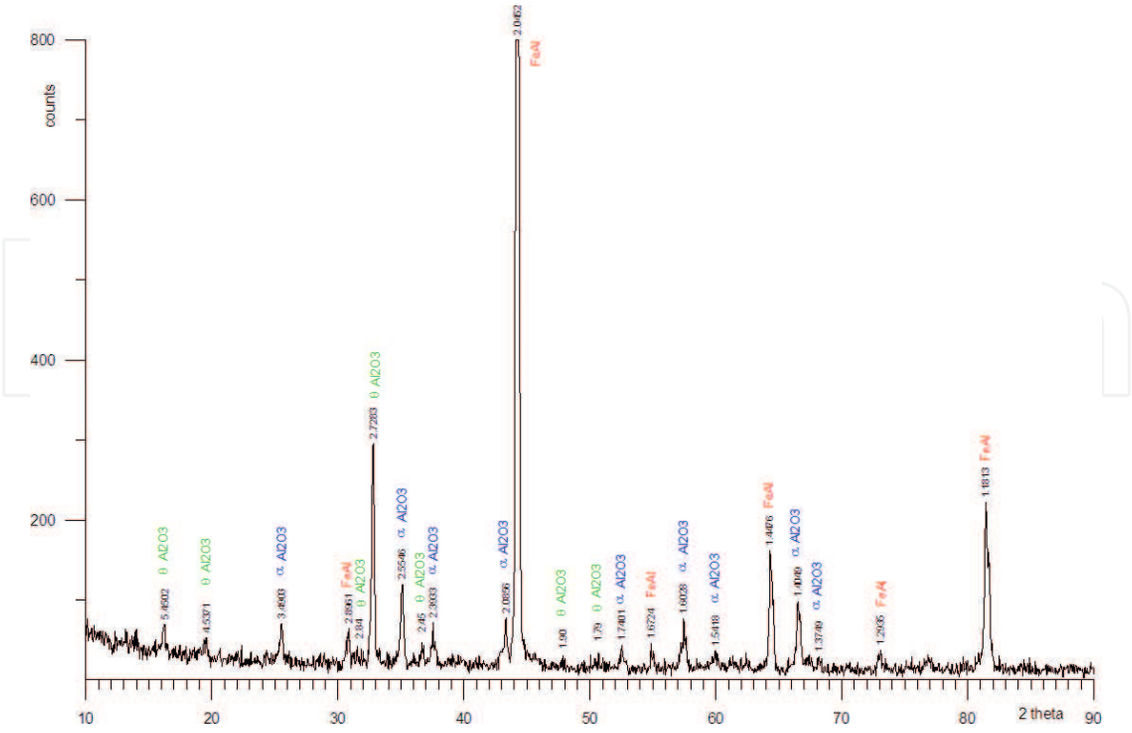

Figure 11. X-ray diffraction of the products of corrosion of the sample after oxidation at the temperature 1173 K in time 48 h.

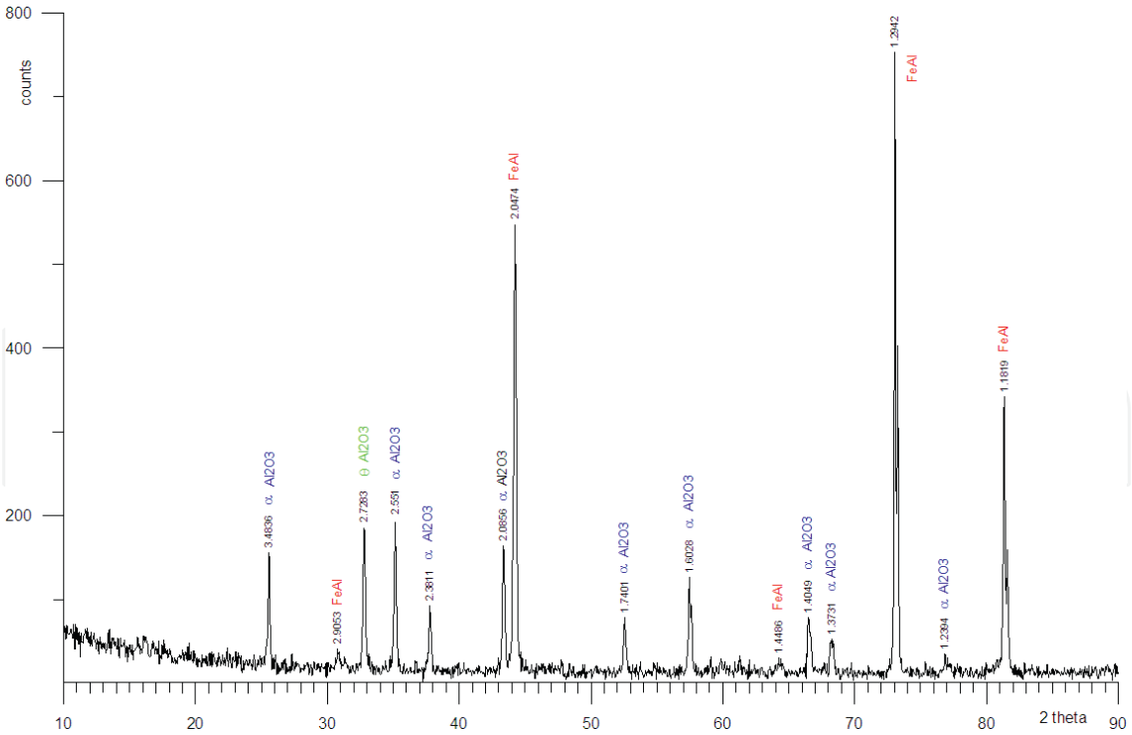

Figure 12. X-ray diffraction of the products of corrosion of the sample after oxidation at the temperature 1273 K in time 48 h.

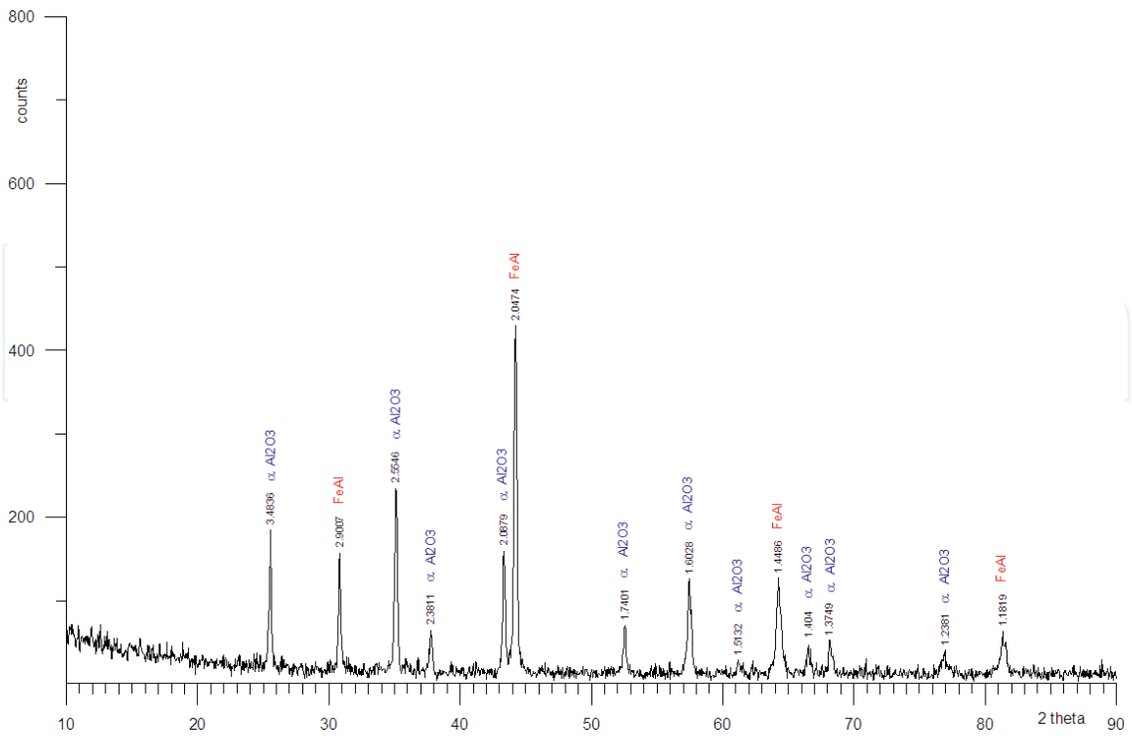

Figure 13. X-ray diffraction of the products of corrosion of the sample after oxidation at the temperature 1373 K in time 48 h.

3. The thickness of the corrosive layer

The kinetics of the corrosion process and the parabolic constant of the oxidation process (k_p) were the basis for determining the thickness of the corrosive layer. The k_p values for temperatures of 1173, 1223, 1273, 1373 K were calculated from the relation (Eq. (2)):

$$k_p'' - \ constant\ rate\ of\ oxidation, \left(g^2 \cdot cm^{-4} \cdot s^{-1}\right)$$
$$\left(\frac{\Delta m}{s}\right)^2 - weight\ change\ \left(\frac{g2}{cm^4}\right)\ \ t - time\ (s) \tag{2}$$

The results obtained for individual oxidation times are presented in **Table 2**.

Taking into account the corrosion kinetics and the oxygen density of the Al_2O_3 compound, the theoretical thickness of the corrosion layer (based on the oxidation time and process temperature) was calculated. The thickness of the corrosion layer was calculated from the relation (Eq. (3)):

$$\frac{\Delta\, m_O}{s} - weight\ change\ \left(\frac{g}{cm^2}\right) \tag{3}$$

ρ_{Al2O3} = 1.98 g / cm^3 – calculated oxygen density in Al_2O_3 compound, X – layer thickness [cm].

The results of the calculations are shown in **Figure 14**. The real (occurring on the surface) thickness of the corrosion layer is lower because, during its growth, part of this layer comes

http://dx.doi.org/10.5772/intechopen.73184

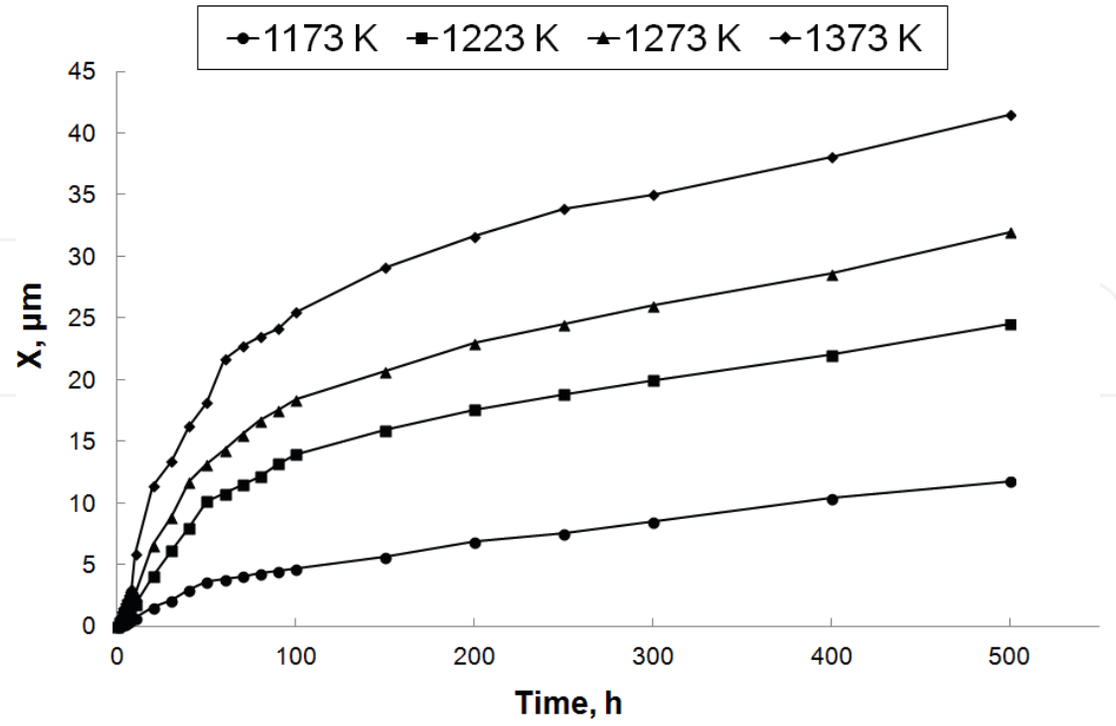

Figure 14. Diagram of the layer thickness calculated from the density of oxygen in Al_2O_3 compound for the time of 500 h.

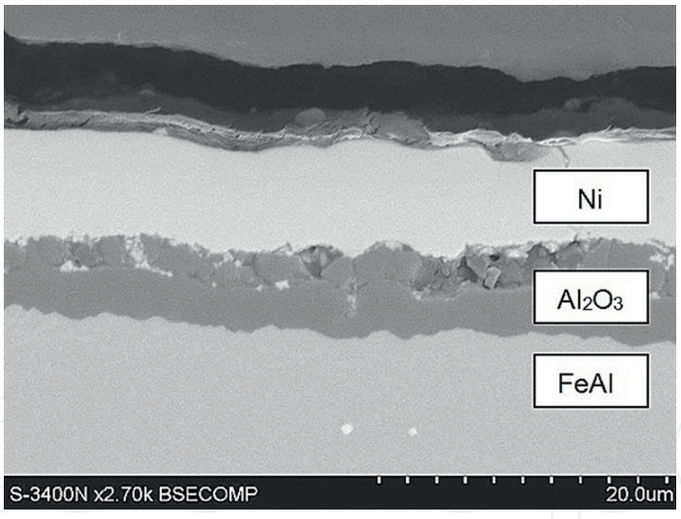

Figure 15. The Al_2O_3 layer after corrosion tests at temperature 1173 K in time 500 h.

off due to different coefficients of thermal expansion of the substrate and corrosion products. **Figures 15** and **16** show a cross-sectional image of a sample after corrosion tests. In order to protect the corrosion layer, the surface was covered with nickel (**Figure 15**). It has been shown that the corrosion layer consists of an area coherently adjacent to the substrate when tested at a temperature of 1173 K for 500 h and a corrosive layer inconsistent with numerous discontinuities for samples subjected to corrosion testing at 1373 K. This phenomenon does not depend on the process time.

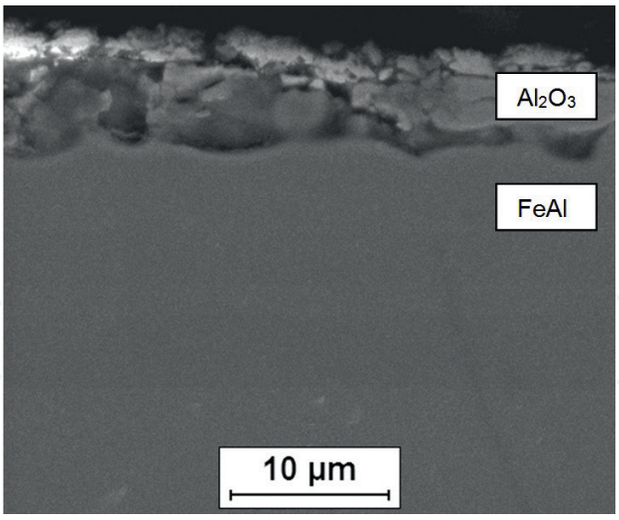

Figure 16. The Al_2O_3 layer after corrosion tests at 1373 K in time 100 h.

3. The operating tests on the intermediate phase of FeAl

Many Fe40Al alloy tests have shown its high resistance to high temperature corrosion in environment rich in chlorine and sulfur compounds. This confirms the possibility of using these materials for elements operating at high temperatures in the atmosphere of exhaust and industrial gases. The high-temperature strength of FeAl alloys is better than the strength of polymer composites and typically used aluminum alloys, so FeAl Fe alloys can be used on rotating elements [24]. Such conditions occur for example in turbochargers of car engines.

Turbochargers are one of the basic components of an internal combustion engine that influence its parameters. They consist of a turbine (the so-called hot part), driven on the flue side and a compressor (so-called cold part) on the compressed air side, set on a common shaft. The rotating assembly is the main element of its structure, which is held in the central body with plain bearings [25].

Due to high temperature of operating turbine, the basic issue is the selection of a material resistant to high temperatures, oxidation, aggressive working environment and creep (deformation). The exhaust gas temperature of the compression-ignition engine is about 973 K, and for spark-ignition engines it can be over 1273 K.

Due to the high temperature of exhaust gas and continuous changes of pressure, as well as a high rotational speed of up to 200 000 rpm it is necessary to use heat resistant materials [26, 27].

The durability of the turbocharger is also influenced by the presence of impurities entering the interior of the intake system, exhaust system and lubrication, and therefore the materials used for its components should exhibit abrasion resistance [28].

Taking into account the properties of alloys on the FeAl alloy phase and the working conditions and material requirements of turbochargers, studies have been undertaken to determine the feasibility of the use of Fe40Al5Cr0.2TiB intermetallic alloys for components of the hot parts of turbocharger of a car with a compression ignition engine.

The tests were performed on the Fe40Al5Cr0.2TiB intermetallic alloy which has been used as a material for making the axles of rollers for pressure control system in the suction manifold and the sleeve at the sealing ring of the turbocharger impeller (**Figures 17**, **18**). These elements are made of Fe40Al5Cr0.2TiB intermetallic alloy. The turbocharger was operated in road conditions for a distance of 80 000 km. After the tests, the turbocharger was dismantled and the components of the Fe40Al5Cr0.2TiB intermetallic alloy were tested.

The comparison of appearance of surface elements made from intermetallic Fe40Al5Cr0.2TiB alloy, after operating at a distance of 80 000 km indicates that there are no signs of tribological wear on them, and the surface is damage free.

The study of the rolls axis surface after their lifetime has been done with Hitachi S-4200 electronic scanning microscope. On the rollers surface small amounts of corrosion products and so-called carbon deposit (compounds derived from burnt engine oil) were found. The presence of single surface inequalities, which may be the result of the occurrence of metallurgical faults of the type of rupture, was also shown (**Figures 19**, **20**).

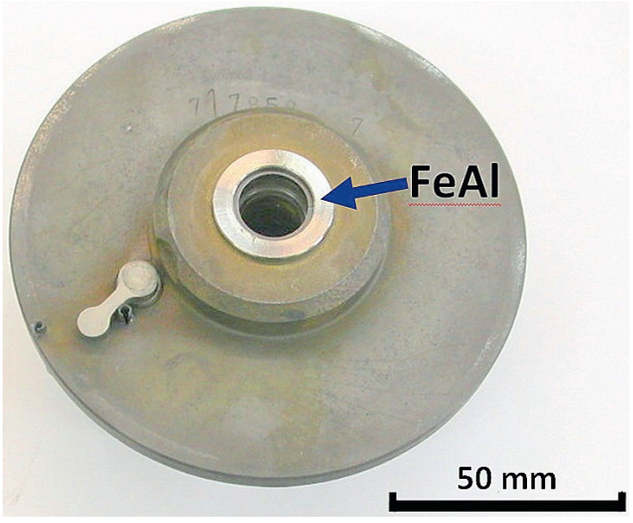

Figure 17. Turbine lid. The arrow indicates the sealing made of the alloy based on FeAl intermetallic phase matrix.

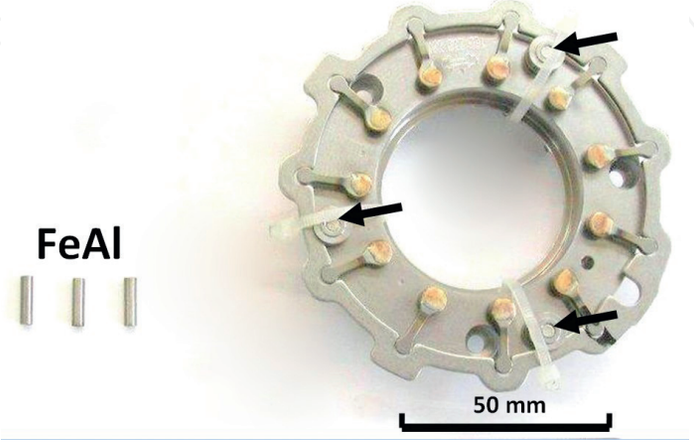

Figure 18. The axles of the pressure control regulator rollers before the test and the place in embedded.

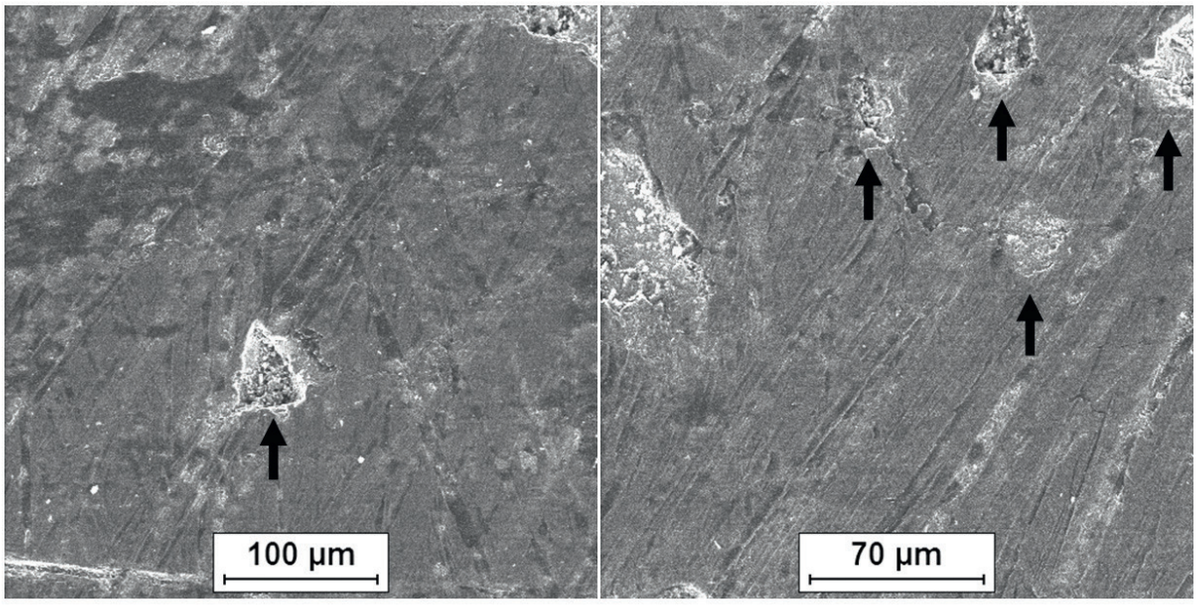

Figure 19. Surface view of the roll axis control system made Fe40Al5Cr0.2TiB intermetallic alloy. Visible metallurgical defects in the form of shrinkage porosity.

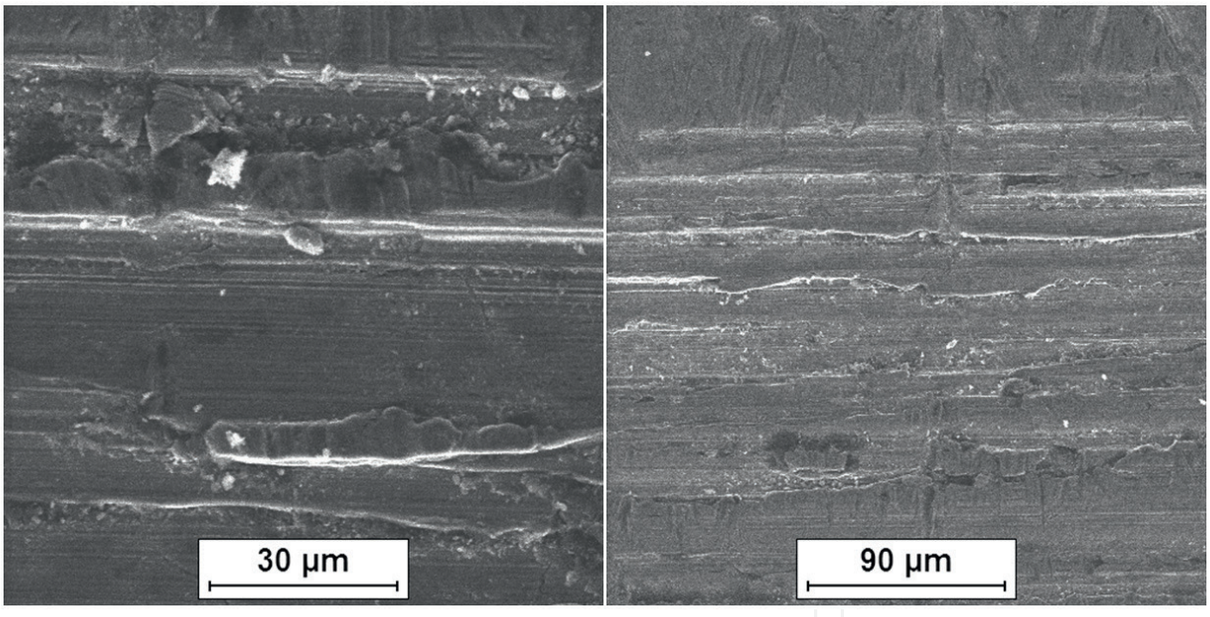

Figure 20. Surface of the roller axle of the control unit made of intermetallic alloy Fe40Al5Cr0.2TiB.

The turbocharger operating conditions (high temperature, corrosive environment) make the turbocharger one of the most unreliable components of the engine. This failure can be reduced by using modern materials, including alloys based on FeAl's intermetallic phase.

In the research, the tests of application FeAl alloys on the axle of the variable-geometry steering wheel control vanes were made. Conventional solutions often cause the turbocharger to malfunction due to the clogging of the rollers and their mounting axles, resulting in the lack of proper pressure control in the suction manifold. The use of FeAl alloys on the exhaust control

rollers axis was characterized by the correct operation of a turbocharger operated under high engine load conditions over a distance 80,000 km.

Determining the predictable lifetime of alloys based on FeAl's intermetallic phase as heat-resistant components working in the hot turbocharger section requires further investigation in this field, including verification for longer operating distances.

4. Summary

Summarizing the description of the processes involved in the high temperature corrosion of FeAl alloys, it seems appropriate to analyze key achievements concerning this issue in recent years.

Protecting metals from oxidation at high temperatures is one of the important problems of modern technology. Understanding the rate of process under certain conditions is essential both in theory and in practice. The phenomenon of gas corrosion is a source of many serious technical problems due to the large number of different technological processes running at high temperatures. The process which is limiting the growth of the protective oxide scale is volumetric diffusion. In industrial conditions we usually deal with different atmospheres, often very of variable composition, and also with non-isothermal conditions.

The possibility of reaction on metal surfaces and the composition of gas corrosion products can be predicted on the basis of thermodynamic data. Oxidation of metals of good heat-resistance is a type of evenly spread corrosion that is uniform across the entire surface to produce a layer of products having the same thickness throughout the corroded area. The rate of corrosion is most often determined by the growth of the mass of the sample or the volume of obtained products or spent gas substitutions calculated per unit of surface of the corroding metal surface, sometimes by determining the reaction rate of the reaction zone (depth of the corrosion zone) [29, 30]. When analyzing the kinetics of the metal oxidation process, it is important to define the kinetic law that the process follows and also to determine the reaction rate. The activation energy of the oxidation process (determined from kinetic measurements) is the energy of the slowest-running partial process, which determines the speed of the scale growth. It is assumed that the primary requirement for the oxide layer is to be airtight and to protect the metal from further corrosion is its greater volume relative to the volume of metal from which the oxide is formed, in accordance with the Pilling-Bedworth rule.

In case of large differences in volume, strong stresses, layer cracks and rapid oxygen diffusion paths may occur [31, 32]. Oxidation studies based on intermetallic compounds from the Fe-Al system show that a continuous layer of aluminum oxide forms on the surface of the coatings. Such an α-Al_2O_3 oxide layer generated on the coatings during cyclic oxidation at 1373 K and 100 h shows significantly better corrosion resistance than θ-Al_2O_3 oxide produced on the alloy surface of the FeAl alloy [33].

FeAl alloys should be used for construction materials, protective coatings and materials working in high-temperature corrosion conditions. The high-temperature strength of FeAl alloys is better than composites and used aluminum alloys, thus FeAl alloys can be used on spinning components [24].

Studies have shown that the growth of α-Al_2O_3 scale occurs with the involvement of oxygen transport at the intracellular boundaries in the oxide. Because of the low concentration of point defects in the α-Al_2O_3 phase, the network diffusion of aluminum and oxygen in this oxide is not included in the mass balance sheet by the corrosion product layer [22, 23]. The calculations and experiments carried out show that aluminum transport in the absence of contact of corrosion products with melt substrate (pore occurrence) occurs by the aluminum alloy evaporation. It is sufficient for the formation of oxide. X-rays showed that at 1373 K after 48 h α-Al_2O_3 is the dominant component of the scale.

Taking into account the properties of the FeAl alloy, the working conditions and material requirements of the turbochargers, studies have been carried out to determine the feasibility of the use of the Fe40Al5Cr0.2TiB intermetallic alloy for hot-dipped turbocharger components. Axis of the pressure control rollers in the suction manifold and the sleeve at the sealing ring of the turbocharger rotor ring were made. Operation was performed under extreme turbocharger operation conditions (high load engine operation). The conditions produced during the test often lead to a turbocharger failure, which results in damage to the exhaust control system due to the seizure of the control mechanism. Performance tests have yielded a positive result, preserving turbocharger performance for 80 000 km.

5. Conclusion

1. The kinetics of the corrosion process of the high temperature alloy Fe40Al5Cr0.2TiB after the incubation period is in accordance with the parabolic law. Deviations from the parabolic course in the initial period are due to the fact that different allotropic variants of Al_2O_3 oxide and grain growth occur.

2. The α-Al_2O_3 scale formed on the surface is characterized by different thermal expansion compared to the thermal expansion of the FeAl phase. Diffusion of the thermal expansion coefficient results in the formation of microcracks in the case of cyclic reduction and temperature rise, leading to the falling of the protective oxide layer. The rate of growth of the scale in places where it has lost contact with the alloy (porosity) is the same as where the contact was maintained.

3. In the multicomponent alloy Fe40Al5Cr0.2TiB corrosion products formed on the surface of the material in the temperature range 1273 -1373 K the dominant oxide is α-Al_2O_3. The proportion of other oxides, e.g. Cr_2O_3, is negligible. This is due to the fact that the oxides of the remaining elements in the alloy, such as iron, chromium, have several orders of magnitude higher decomposition. For this reason Al in the Fe40Al5Cr0.2TiB alloy is selectively oxidized to form stable α-Al2O3 oxide on the melt surface.

4. Morphology and phase composition of the scale are characterized by differentiation depending on the temperature at which the oxidation process takes place. In the temperature range up to 1223 K, metastable θ oxides are observed. Over time, the crystallographic network rebuilds to the α-Al_2O_3 phase. At higher temperatures, the time at which the continuous α-Al_2O_3 layer is produced decreases. Only α-Al_2O_3 phase was observed at 1373 K after 48 h.

5. The thickness of the corrosion layer determined on the basis of the kinetics of the discontinuous process shows differentiation compared to the results of thermogravimetric measurements. The thickness of the corrosion layer measured on the surface of the oxidized samples in the crucibles is lower, as it decays during the cooling process due to the different coefficients of thermal expansion of the substrate.

6. The use of the Fe40Al5Cr0.2TiB intermetallic alloy for hot turbocharger parts as nickel alloy alternatives with compression ignition has allowed operation while preserving the nominal compressor characteristics during the entire operating test. Surface condition tests carried out on elements after the course of 80 000 km showed no signs of tribological wear and the surface of these elements was free of corrosion damage.

Acknowledgements

During the implementation of the research, the knowledge and experience of the employees of the Faculty of Materials Science and Ceramics of the Department of Physicochemistry and Process Modeling of the AGH University of Science and Technology were used. I sincerely thank Prof. PhD Eng. Marek Danielewski for help in carrying out research.

Author details

Janusz Cebulski and Dorota Pasek*

*Address all correspondence to: dorota.pasek@polsl.pl

Silesian University of Technology, Katowice, Poland

References

[1] Jóźwiak S. Aluminki żelaza. Sekwencja przemian fazowych w procesie nieizotermicznego spiekania proszków żelaza i aluminium. Bel Studio, Warszawa; 2014

[2] Deevi SC, Sikka VK. Nickel and iron aluminides: An overview on properties, processing, and applications. Intermetallics. 1996;**4**:357-375

[3] Liu CT, Stringer J, Mundy JN, Horton LL, Angelini P. Ordered intermetallic alloys: An assessment. Intermetallics. 1997;**5**:579-596

[4] Sikka VK, Wilkening D, Liebetrau J, Mackey B. Melting and casting of FeAl-based cast alloy. Materials Science and Engineering. 1998;**A258**:229-235

[5] Formanek B, Szczucka-Lasota B. Odporność na korozję wysoko-temperaturową stopów międzymetalicznych z układu Fe-Al. Ochrona przed korozją. 2009;**513**:583-588

[6] Bystrzycki J, Varm RA, Bojar Z. Postępy w badaniach stopów na bazie uporządkowanych faz międzymetalicznych z udziałem aluminium. Inżynieria Materiałowa. 1996;**5**:137

[7] Schmitta A, Kumarb KS, Kauffmanna A, Lic X, Steinc F, Heilmaiera M. Creep of binary Fe-Al alloys with ultrafine lamellar microstructures. Intermetallics. 2017;**90**:180-187

[8] Cebulski J. Sposoby podwyższania plastyczności stopu na osnowie związku międzymetalicznego FeAl. Rozprawa doktorska. Gliwice: Politechnika Śląska; 1998

[9] Schindler I, Kratochvíl P, Prokopčáková P, Kozelský P. Forming of caste Fe – 45at.% Al alloy with high content of carbon. Intermetallics. 2010;**18**:745-747

[10] Barcik J, Cebulski J. Plastify of alloy based on the matrix of intermetallic FeAl phase. Archives of Metallurgy. 2000;**45**(3):315-330

[11] Grabke HJ. Oxidation of NiAl and FeAl. Intermetallics. 1999;**7**:1153-1158

[12] Danng Ngoc Chan C, Huvier C, Dinhut JF. High temperature corrosion of some B2 iron aluminides. Intermetallics. 2001;**9**:817-826

[13] Formanek B, Szymański K, Beliayev A: Composite carbide powders and HVOF sprayed coatings with a plastic matrix. Journal of Achievements in Materials and Manufacturing Engineering. 2006;**13**(1/2):351-354

[14] Cebulski J, Tytko K. Przeróbka plastyczna metodą wyciskania zwłaszcza stopów na osnowie fazy międzymetalicznej FeAl. Patent No. 208310, decyzja Urzędu Patentowego Rzeczypospolitej Polskiej z dnia Nov 26, 2010

[15] Cebulski J. Żaroodporność stopów na osnowie fazy międzymetalicznej FeAl, Wydawnictwo Politechniki Śląskiej, Gliwice. 2014

[16] Mrowec S. Teoria dyfuzji w stanie stałym. Warszawa: Państwowe Wydawnictwo Naukowe; 1989

[17] Brumm W, Grabke HJ. The oxidation behaviour of NiAl-I. Phase transformations in the alumina scale during oxidation of NiAl an NiAl-Cr alloys. Corrosion Science. 1992;**33**:1677-1690

[18] Schumann E. The effect of Y-ion implantation on the oxidation of β-NiAl. Oxidation of Metals. 1995;**43**:157-172

[19] Young JC, Schumann E, Levin I, Ruhle M. Transient oxidation of NiAl. Acta Materiala. 1998;**46**:2195-2201

[20] Hindam HM, Smeltzer WW. Growth and Microstructure of α - Al_2O_3 on Ni-Al Alloys: Internal Precipitation and Transition to External Scale. Journal on the Electrochemical Society. 1980;**127**(7):1622-1630

[21] Doychak J, Ruhle M. TEM studies of oxidized NiAl and Ni_3Al cross sections. Oxidation of Metals. 1989;**31**:431-452

[22] Clemens D, Bongartz K, Speier W, Hussey RJ, Quadakkers WJ. Analysis and modelling of transport processes in alumina scales on high temperature alloys. Fresenius' Journal of Analytical Chemistry. 1993;**346**;318-322

[23] Clements D, Bongartz K, Quadakkers WJ, Nickel H, Holzbrecher H, Becker JS. Determination of lattice and grain boundary diffusion coefficients in protective alumina scales on high temperature alloys using SEM, TEM and SIMS. Fresenius' Journal of Analytical Chemistry. 1995;**353**:267-270

[24] Kupka M. Technological plasticity studies of the FeAl intermetallic phase-based alloy. Intermetallics. 2004;**12**:295-302

[25] Schweizer B, Sievert M. Noulinear oscillations of automotive turbocharger turbines. Journal of Sound and Vibration. 2009;**321**:955-975

[26] Romagnoli A, Martinez-Botas R. Heat transfer analysis in a turbocharger turbine: An experimental and computational evaluation. Applied Thermal Engineering. 2012;**38**:58-77

[27] Tetsui T. Development of TiAl turbocharger for passenger vehicle. Materials Science and Engineering. 2002;**A329-331**:582-588

[28] Pint BA, Haynes JA, Armstrong BL. Performance of advanced turbocharger alloys and coatings at 850-950°C in air with water vapor. Surface & Coatings Technology. 2013; **215**:90-95

[29] Jabłońska M, Jasik A, Hanc A. Structure and some mechanical properties of Fe(3) Al-based cast alloys. Archives of Metallurgy and Materials. 2009;**54**(3):731-739

[30] Formanek B, Hernas A, et al. Structre and Applications, Materials Week. International Congres on Advanced Materials, their Processes and Applications, Monachium. 2000

[31] Cebulski J. Odporność korozyjna stopów na osnowie fazy międzymetalicznej FeAl po krystalizacji i po przeróbce plastycznej. Hutnik-Wiadomości Hutnicze. 2012;**8**:557-561

[32] Cebulski J, Lalik S, Michalik R. Corrosion resistance of FeAl intermetallic phase based alloy in water solution of NaCl. Journal of Achievements in Materials and Manufacturing Engineering. 2008; **27**:15-18

[33] Hernas A, Piliszko B, Imosa M. Resistance to high-temperature corrosion of new materials for power industry. Archiwum Combustionis. PAN. 2007;**27**(1):4-7

IntechOpen